

Transverse momentum and centrality dependence of dihadron correlations in Au+Au collisions at $\sqrt{s_{\text{NN}}} = 200$ GeV: Jet-quenching and the response of partonic matter

A. Adare,⁸ S. Afanasiev,²² C. Aidala,⁹ N.N. Ajitanand,⁴⁹ Y. Akiba,^{43,44} H. Al-Bataineh,³⁸ J. Alexander,⁴⁹ A. Al-Jamel,³⁸ K. Aoki,^{28,43} L. Aphecetche,⁵¹ R. Armendariz,³⁸ S.H. Aronson,³ J. Asai,⁴⁴ E.T. Atomssa,²⁹ R. Averbeck,⁵⁰ T.C. Awes,³⁹ B. Azmoun,³ V. Babintsev,¹⁸ G. Baksay,¹⁴ L. Baksay,¹⁴ A. Baldissieri,¹¹ K.N. Barish,⁴ P.D. Barnes,³¹ B. Bassalleck,³⁷ S. Bathe,⁴ S. Batsouli,^{9,39} V. Baublis,⁴² F. Bauer,⁴ A. Bazilevsky,³ S. Belikov,^{3,21} R. Bennett,⁵⁰ Y. Berdnikov,⁴⁶ A.A. Bickley,⁸ M.T. Bjorndal,⁹ J.G. Boissevain,³¹ H. Borel,¹¹ K. Boyle,⁵⁰ M.L. Brooks,³¹ D.S. Brown,³⁸ D. Bucher,³⁴ H. Buesching,³ V. Bumazhnov,¹⁸ G. Bunce,^{3,44} J.M. Burward-Hoy,³¹ S. Butsyk,^{31,50} S. Campbell,⁵⁰ J.-S. Chai,²³ B.S. Chang,⁵⁸ J.-L. Charvet,¹¹ S. Chernichenko,¹⁸ J. Chiba,²⁴ C.Y. Chi,⁹ M. Chiu,^{9,19} I.J. Choi,⁵⁸ T. Chujo,⁵⁵ P. Chung,⁴⁹ A. Churyn,¹⁸ V. Cianciolo,³⁹ C.R. Clevén,¹⁶ Y. Cobigo,¹¹ B.A. Cole,⁹ M.P. Comets,⁴⁰ P. Constantin,^{21,31} M. Csanád,¹³ T. Csörgő,²⁵ T. Dahms,⁵⁰ K. Das,¹⁵ G. David,³ M.B. Deaton,¹ K. Dehmelt,¹⁴ H. Delagrangé,⁵¹ A. Denisov,¹⁸ D. d'Enterria,⁹ A. Deshpande,^{44,50} E.J. Desmond,³ O. Dietzsch,⁴⁷ A. Dion,⁵⁰ M. Donadelli,⁴⁷ J.L. Drachenberg,¹ O. Drapier,²⁹ A. Drees,⁵⁰ A.K. Dubey,⁵⁷ A. Durum,¹⁸ V. Dzhordzhadze,^{4,52} Y.V. Efremenko,³⁹ J. Egdemir,⁵⁰ F. Ellinghaus,⁸ W.S. Emam,⁴ A. Enokizono,^{17,30} H. En'yo,^{43,44} B. Espagnon,⁴⁰ S. Esumi,⁵⁴ K.O. Eyster,⁴ D.E. Fields,^{37,44} M. Finger,^{5,22} F. Fleuret,²⁹ S.L. Fokin,²⁷ B. Forestier,³² Z. Fraenkel,⁵⁷ J.E. Frantz,^{9,50} A. Franz,³ A.D. Frawley,¹⁵ K. Fujiwara,⁴³ Y. Fukao,^{28,43} S.-Y. Fung,⁴ T. Fusayasu,³⁶ S. Gadrat,³² I. Garishvili,⁵² F. Gastineau,⁵¹ M. Germain,⁵¹ A. Glenn,^{8,52} H. Gong,⁵⁰ M. Gonin,²⁹ J. Gosset,¹¹ Y. Goto,^{43,44} R. Granier de Cassagnac,²⁹ N. Grau,²¹ S.V. Greene,⁵⁵ M. Grosse Perdekamp,^{19,44} T. Gunji,⁷ H.-Å. Gustafsson,³³ T. Hachiya,^{17,43} A. Hadj Henni,⁵¹ C. Haegemann,³⁷ J.S. Haggerty,³ M.N. Hagiwara,¹ H. Hamagaki,⁷ R. Han,⁴¹ H. Harada,¹⁷ E.P. Hartouni,³⁰ K. Haruna,¹⁷ M. Harvey,³ E. Haslum,³³ K. Hasuko,⁴³ R. Hayano,⁷ M. Heffner,³⁰ T.K. Hemmick,⁵⁰ T. Hester,⁴ J.M. Heuser,⁴³ X. He,¹⁶ H. Hiejima,¹⁹ J.C. Hill,²¹ R. Hobbs,³⁷ M. Hohlmann,¹⁴ M. Holmes,⁵⁵ W. Holzmann,⁴⁹ K. Homma,¹⁷ B. Hong,²⁶ T. Horaguchi,^{43,53} D. Hornback,⁵² M.G. Hur,²³ T. Ichihara,^{43,44} K. Imai,^{28,43} M. Inaba,⁵⁴ Y. Inoue,^{45,43} D. Isenhower,¹ L. Isenhower,¹ M. Ishihara,⁴³ T. Isobe,⁷ M. Issah,⁴⁹ A. Isupov,²² B.V. Jacak,^{50,*} J. Jia,⁹ J. Jin,⁹ O. Jinnouchi,⁴⁴ B.M. Johnson,³ K.S. Joo,³⁵ D. Jouan,⁴⁰ F. Kajihara,^{7,43} S. Kametani,^{7,56} N. Kamihara,^{43,53} J. Kamin,⁵⁰ M. Kaneta,⁴⁴ J.H. Kang,⁵⁸ H. Kanou,^{43,53} T. Kawagishi,⁵⁴ D. Kwall,⁴⁴ A.V. Kazantsev,²⁷ S. Kelly,⁸ A. Khanzadeev,⁴² J. Kikuchi,⁵⁶ D.H. Kim,³⁵ D.J. Kim,⁵⁸ E. Kim,⁴⁸ Y.-S. Kim,²³ E. Kinney,⁸ A. Kiss,¹³ E. Kistenev,³ A. Kiyomichi,⁴³ J. Klay,³⁰ C. Klein-Boesing,³⁴ L. Kochenda,⁴² V. Kochetkov,¹⁸ B. Komkov,⁴² M. Konno,⁵⁴ D. Kotchetkov,⁴ A. Kozlov,⁵⁷ A. Král,¹⁰ A. Kravitz,⁹ P.J. Kroon,³ J. Kubart,^{5,20} G.J. Kunde,³¹ N. Kurihara,⁷ K. Kurita,^{45,43} M.J. Kweon,²⁶ Y. Kwon,^{52,58} G.S. Kyle,³⁸ R. Lacey,⁴⁹ Y.-S. Lai,⁹ J.G. Lajoie,²¹ A. Lebedev,²¹ Y. Le Bornec,⁴⁰ S. Leckey,⁵⁰ D.M. Lee,³¹ M.K. Lee,⁵⁸ T. Lee,⁴⁸ M.J. Leitch,³¹ M.A.L. Leite,⁴⁷ B. Lenzi,⁴⁷ H. Lim,⁴⁸ T. Liška,¹⁰ A. Litvinenko,²² M.X. Liu,³¹ X. Li,⁶ X.H. Li,⁴ B. Love,⁵⁵ D. Lynch,³ C.F. Maguire,⁵⁵ Y.I. Makdisi,³ A. Malakhov,²² M.D. Malik,³⁷ V.I. Manko,²⁷ Y. Mao,^{41,43} L. Mašek,^{5,20} H. Masui,⁵⁴ F. Matathias,^{9,50} M.C. McCain,¹⁹ M. McCumber,⁵⁰ P.L. McGaughey,³¹ Y. Miake,⁵⁴ P. Mikeš,^{5,20} K. Miki,⁵⁴ T.E. Miller,⁵⁵ A. Milov,⁵⁰ S. Mioduszewski,³ G.C. Mishra,¹⁶ M. Mishra,² J.T. Mitchell,³ M. Mitrovski,⁴⁹ A. Morreale,⁴ D.P. Morrison,³ J.M. Moss,³¹ T.V. Moukhanova,²⁷ D. Mukhopadhyay,⁵⁵ J. Murata,^{45,43} S. Nagamiya,²⁴ Y. Nagata,⁵⁴ J.L. Nagle,⁸ M. Naglis,⁵⁷ I. Nakagawa,^{43,44} Y. Nakamiya,¹⁷ T. Nakamura,¹⁷ K. Nakano,^{43,53} J. Newby,³⁰ M. Nguyen,⁵⁰ B.E. Norman,³¹ A.S. Nyanin,²⁷ J. Nystrand,³³ E. O'Brien,³ S.X. Oda,⁷ C.A. Ogilvie,²¹ H. Ohnishi,⁴³ I.D. Ojha,⁵⁵ H. Okada,^{28,43} K. Okada,⁴⁴ M. Oka,⁵⁴ O.O. Omiwade,¹ A. Oskarsson,³³ I. Otterlund,³³ M. Ouchida,¹⁷ K. Ozawa,⁷ R. Pak,³ D. Pal,⁵⁵ A.P.T. Palounek,³¹ V. Pantuev,⁵⁰ V. Papavassiliou,³⁸ J. Park,⁴⁸ W.J. Park,²⁶ S.F. Pate,³⁸ H. Pei,²¹ J.-C. Peng,¹⁹ H. Pereira,¹¹ V. Peresedov,²² D.Yu. Peressounko,²⁷ C. Pinkenburg,³ R.P. Pisani,³ M.L. Purschke,³ A.K. Purwar,^{31,50} H. Qu,¹⁶ J. Rak,^{21,37} A. Rakotozafindrabe,²⁹ I. Ravinovich,⁵⁷ K.F. Read,^{39,52} S. Rembeczki,¹⁴ M. Reuter,⁵⁰ K. Reyggers,³⁴ V. Riabov,⁴² Y. Riabov,⁴² G. Roche,³² A. Romana,^{29,†} M. Rosati,²¹ S.S.E. Rosendahl,³³ P. Rosnet,³² P. Rukoyatkin,²² V.L. Rykov,⁴³ S.S. Ryu,⁵⁸ B. Sahlmueller,³⁴ N. Saito,^{28,43,44} T. Sakaguchi,^{3,7,56} S. Sakai,⁵⁴ H. Sakata,¹⁷ V. Samsonov,⁴² H.D. Sato,^{28,43} S. Sato,^{3,24,54} S. Sawada,²⁴ J. Seele,⁸ R. Seidl,¹⁹ V. Semenov,¹⁸ R. Seto,⁴ D. Sharma,⁵⁷ T.K. Shea,³ I. Shein,¹⁸ A. Shevel,^{42,49} T.-A. Shibata,^{43,53} K. Shigaki,¹⁷ M. Shimomura,⁵⁴ T. Shohjoh,⁵⁴ K. Shoji,^{28,43} A. Sickles,⁵⁰ C.L. Silva,⁴⁷ D. Silvermyr,³⁹ C. Silvestre,¹¹ K.S. Sim,²⁶ C.P. Singh,² V. Singh,² S. Skutnik,²¹ M. Slunečka,^{5,22} W.C. Smith,¹ A. Soldatov,¹⁸ R.A. Soltz,³⁰ W.E. Sondheim,³¹ S.P. Sorensen,⁵² I.V. Sourikova,³ F. Staley,¹¹ P.W. Stankus,³⁹ E. Stenlund,³³ M. Stepanov,³⁸ A. Ster,²⁵ S.P. Stoll,³ T. Sugitate,¹⁷ C. Suire,⁴⁰

J.P. Sullivan,³¹ J. Sziklai,²⁵ T. Tabaru,⁴⁴ S. Takagi,⁵⁴ E.M. Takagui,⁴⁷ A. Taketani,^{43,44} K.H. Tanaka,²⁴ Y. Tanaka,³⁶ K. Tanida,^{43,44} M.J. Tannenbaum,³ A. Taranenko,⁴⁹ P. Tarján,¹² T.L. Thomas,³⁷ M. Togawa,^{28,43} A. Toia,⁵⁰ J. Tojo,⁴³ L. Tomášek,²⁰ H. Torii,⁴³ R.S. Towell,¹ V-N. Tram,²⁹ I. Tserruya,⁵⁷ Y. Tsuchimoto,^{17,43} S.K. Tuli,² H. Tydesjö,³³ N. Tyurin,¹⁸ C. Vale,²¹ H. Valle,⁵⁵ H.W. van Hecke,³¹ J. Velkovska,⁵⁵ R. Vertesi,¹² A.A. Vinogradov,²⁷ M. Virius,¹⁰ V. Vrba,²⁰ E. Vznuzdaev,⁴² M. Wagner,^{28,43} D. Walker,⁵⁰ X.R. Wang,³⁸ Y. Watanabe,^{43,44} J. Wessels,³⁴ S.N. White,³ N. Willis,⁴⁰ D. Winter,⁹ C.L. Woody,³ M. Wysocki,⁸ W. Xie,^{4,44} Y. Yamaguchi,⁵⁶ A. Yanovich,¹⁸ Z. Yasin,⁴ J. Ying,¹⁶ S. Yokkaichi,^{43,44} G.R. Young,³⁹ I. Younus,³⁷ I.E. Yushmanov,²⁷ W.A. Zajc,⁹ O. Zaudtke,³⁴ C. Zhang,^{9,39} S. Zhou,⁶ J. Zimányi,^{25,†} and L. Zolin²²

(PHENIX Collaboration)

¹Abilene Christian University, Abilene, TX 79699, U.S.

²Department of Physics, Banaras Hindu University, Varanasi 221005, India

³Brookhaven National Laboratory, Upton, NY 11973-5000, U.S.

⁴University of California - Riverside, Riverside, CA 92521, U.S.

⁵Charles University, Ovocný trh 5, Praha 1, 116 36, Prague, Czech Republic

⁶China Institute of Atomic Energy (CIAE), Beijing, People's Republic of China

⁷Center for Nuclear Study, Graduate School of Science, University of Tokyo, 7-3-1 Hongo, Bunkyo, Tokyo 113-0033, Japan

⁸University of Colorado, Boulder, CO 80309, U.S.

⁹Columbia University, New York, NY 10027 and Nevis Laboratories, Irvington, NY 10533, U.S.

¹⁰Czech Technical University, Zikova 4, 166 36 Prague 6, Czech Republic

¹¹Dapnia, CEA Saclay, F-91191, Gif-sur-Yvette, France

¹²Debrecen University, H-4010 Debrecen, Egyetem tér 1, Hungary

¹³ELTE, Eötvös Loránd University, H - 1117 Budapest, Pázmány P. s. 1/A, Hungary

¹⁴Florida Institute of Technology, Melbourne, FL 32901, U.S.

¹⁵Florida State University, Tallahassee, FL 32306, U.S.

¹⁶Georgia State University, Atlanta, GA 30303, U.S.

¹⁷Hiroshima University, Kagamiyama, Higashi-Hiroshima 739-8526, Japan

¹⁸IHEP Protvino, State Research Center of Russian Federation, Institute for High Energy Physics, Protvino, 142281, Russia

¹⁹University of Illinois at Urbana-Champaign, Urbana, IL 61801, U.S.

²⁰Institute of Physics, Academy of Sciences of the Czech Republic, Na Slovance 2, 182 21 Prague 8, Czech Republic

²¹Iowa State University, Ames, IA 50011, U.S.

²²Joint Institute for Nuclear Research, 141980 Dubna, Moscow Region, Russia

²³KAERI, Cyclotron Application Laboratory, Seoul, South Korea

²⁴KEK, High Energy Accelerator Research Organization, Tsukuba, Ibaraki 305-0801, Japan

²⁵KFKI Research Institute for Particle and Nuclear Physics of the Hungarian Academy of Sciences (MTA KFKI RMKI), H-1525 Budapest 114, POBox 49, Budapest, Hungary

²⁶Korea University, Seoul, 136-701, Korea

²⁷Russian Research Center "Kurchatov Institute", Moscow, Russia

²⁸Kyoto University, Kyoto 606-8502, Japan

²⁹Laboratoire Leprince-Ringuet, Ecole Polytechnique, CNRS-IN2P3, Route de Saclay, F-91128, Palaiseau, France

³⁰Lawrence Livermore National Laboratory, Livermore, CA 94550, U.S.

³¹Los Alamos National Laboratory, Los Alamos, NM 87545, U.S.

³²LPC, Université Blaise Pascal, CNRS-IN2P3, Clermont-Fd, 63177 Aubiere Cedex, France

³³Department of Physics, Lund University, Box 118, SE-221 00 Lund, Sweden

³⁴Institut für Kernphysik, University of Muenster, D-48149 Muenster, Germany

³⁵Myongji University, Yongin, Kyonggido 449-728, Korea

³⁶Nagasaki Institute of Applied Science, Nagasaki-shi, Nagasaki 851-0193, Japan

³⁷University of New Mexico, Albuquerque, NM 87131, U.S.

³⁸New Mexico State University, Las Cruces, NM 88003, U.S.

³⁹Oak Ridge National Laboratory, Oak Ridge, TN 37831, U.S.

⁴⁰IPN-Orsay, Université Paris Sud, CNRS-IN2P3, BP1, F-91406, Orsay, France

⁴¹Peking University, Beijing, People's Republic of China

⁴²PNPI, Petersburg Nuclear Physics Institute, Gatchina, Leningrad region, 188300, Russia

⁴³RIKEN, The Institute of Physical and Chemical Research, Wako, Saitama 351-0198, Japan

⁴⁴RIKEN BNL Research Center, Brookhaven National Laboratory, Upton, NY 11973-5000, U.S.

⁴⁵Physics Department, Rikkyo University, 3-34-1 Nishi-Ikebukuro, Toshima, Tokyo 171-8501, Japan

⁴⁶Saint Petersburg State Polytechnic University, St. Petersburg, Russia

⁴⁷Universidade de São Paulo, Instituto de Física, Caixa Postal 66318, São Paulo CEP05315-970, Brazil

⁴⁸System Electronics Laboratory, Seoul National University, Seoul, South Korea

⁴⁹Chemistry Department, Stony Brook University, Stony Brook, SUNY, NY 11794-3400, U.S.

⁵⁰Department of Physics and Astronomy, Stony Brook University, SUNY, Stony Brook, NY 11794, U.S.

⁵¹SUBATECH (Ecole des Mines de Nantes, CNRS-IN2P3, Université de Nantes) BP 20722 - 44307, Nantes, France

⁵²University of Tennessee, Knoxville, TN 37996, U.S.

⁵³Department of Physics, Tokyo Institute of Technology, Oh-okayama, Meguro, Tokyo 152-8551, Japan

⁵⁴Institute of Physics, University of Tsukuba, Tsukuba, Ibaraki 305, Japan

⁵⁵Vanderbilt University, Nashville, TN 37235, U.S.

⁵⁶Waseda University, Advanced Research Institute for Science and Engineering, 17 Kikui-cho, Shinjuku-ku, Tokyo 162-0044, Japan

⁵⁷Weizmann Institute, Rehovot 76100, Israel

⁵⁸Yonsei University, IPAP, Seoul 120-749, Korea

(Dated: November 9, 2018)

Azimuthal angle ($\Delta\phi$) correlations are presented for charged hadrons from dijets for $0.4 < p_T < 10$ GeV/c in Au+Au collisions at $\sqrt{s_{NN}} = 200$ GeV. With increasing p_T , the away-side distribution evolves from a broad to a concave shape, then to a convex shape. Comparisons to $p+p$ data suggest that the away-side can be divided into a partially suppressed “head” region centered at $\Delta\phi \sim \pi$, and an enhanced “shoulder” region centered at $\Delta\phi \sim \pi \pm 1.1$. The p_T spectrum for the “head” region softens toward central collisions, consistent with the onset of jet quenching. The spectral slope for the “shoulder” region is independent of centrality and trigger p_T , which offers constraints on energy transport mechanisms and suggests that the “shoulder” region contains the medium response to energetic jets.

PACS numbers: 25.75.Dw

High transverse momentum (p_T) partons are valuable probes of the high energy density matter created at the Relativistic Heavy-Ion Collider (RHIC). These partons lose a large fraction of their energy in the matter prior to forming hadrons, a phenomenon known as jet-quenching. Such energy loss is predicted to lead to strong suppression of both single- and correlated away-side dihadron yields at high p_T [1], consistent with experimental findings [2, 3]. The exact mechanism for energy loss is not yet understood. Recent results of dihadron azimuthal angle ($\Delta\phi$) correlations have indicated strong modification of the away-side jet [3, 4, 5, 6]. For high p_T hadron pairs, such modification is manifested by a partially suppressed away-side peak at $\Delta\phi \sim \pi$ [3]. This has been interpreted as evidence for the fragmentation of jets that survive their passage through the medium.

For intermediate p_T charged hadron pairs, the away-side jet was observed to peak at $\Delta\phi \sim \pi \pm 1.1$ [4, 5], suggesting that the energy lost by high p_T partons is transported to lower p_T hadrons at angles away from $\Delta\phi \sim \pi$. The proposed mechanisms for such energy transport include medium deflection of hard [7] or shower partons [8], large-angle gluon radiation [9, 10], Cherenkov gluon radiation [11], and “Mach Shock” medium excitations [12].

In this letter we present a detailed “mapping” of the p_T and centrality dependence of away-side jet shapes and yields. These measurements (1) allow a detailed investigation of the jet distributions centered around $\Delta\phi \sim \pi \pm 1.1$ and $\Delta\phi \sim \pi$, (2) provide new insight on the interplay between jet quenching and the response of the medium to the lost energy, and (3) provide new constraints for distinguishing the competing mechanisms for energy transport.

The results presented here are based on minimum-bias (MB) Au+Au and $p+p$ datasets as well as a “pho-

ton” level-1 triggered (PT) $p+p$ dataset [13] collected with the PHENIX detector [14] at $\sqrt{s_{NN}}=200$ GeV, during the 2004-2005 RHIC running periods. The collision vertex z was required to be within $|z| < 30$ cm of the nominal crossing point. The event centrality was determined via the method in Ref. [14]. A total of 840 million Au+Au events were analyzed. Charged particles were reconstructed in the two central arms of PHENIX, each covering -0.35 to 0.35 in pseudo-rapidity and 90° in azimuth. The tracking system consists of the drift chambers and two layers of multi-wire proportional chambers with pad readout (PC1 and PC3), achieving a momentum resolution of $0.7\% \oplus 1.1\% p$ (GeV/c) [2].

Dihadron azimuthal angle correlations are obtained by correlating “trigger” (type A) hadrons with “partner” (type B) hadrons. The MB and PT $p+p$ datasets are used for trigger $p_T < 5$ GeV/c and $p_T > 5$ GeV/c, respectively. To reduce background from decays and conversions, tracks are required to have a matching hit within a $\pm 2.3\sigma$ window in PC3. For $p_T > 4$ GeV/c, additional matching hit at the electromagnetic calorimeter (EMC) was required to suppress background tracks that randomly associate with the PC3 [2]. For triggers with $p_T > 5$ GeV/c, a p_T dependent energy cut in the EMC and a tight $\pm 1.5\sigma$ matching cut at the PC3 were applied to reduce the background to $< 10\%$ [15]. This energy cut greatly reduces PT trigger bias effects. The PT $p+p$ results are consistent with the MB $p+p$ data for trigger $p_T > 5$ GeV/c.

The jet associated partner yield per trigger, $Y_{\text{jet}}(\Delta\phi)$, is obtained from the $\Delta\phi$ correlations as [4, 15]:

$$Y_{\text{jet}} = \left[\frac{N^s(\Delta\phi)}{N^m(\Delta\phi)} - b_0 \left(1 + 2v_2^A v_2^B \cos 2\Delta\phi \right) \right] \frac{\int d\Delta\phi N^m(\Delta\phi)}{2\pi N_A \varepsilon_B} \quad (1)$$

where N_A is the number of triggers, ε_B is the single particle efficiency for partners in the full azimuth and $|\eta| < 0.35$; $N^s(\Delta\phi)$ and $N^m(\Delta\phi)$ are pair distributions

from the same- and mixed-events, respectively. Mixed-event pairs are obtained by selecting partners from different events with similar centrality and vertex. The ε_B values include detector acceptance and reconstruction efficiency, with an uncertainty of $\sim 10\%$ [2, 16]. The harmonic term, $2v_2^A v_2^B \cos 2\Delta\phi$, reflects the elliptic flow modulation of the combinatoric pairs in Au+Au collisions [4]. Values for v_2^A and v_2^B for each centrality class are measured via the reaction plane (RP) method [17] using the Beam-Beam Counters at $3 < |\eta| < 4$. The systematic errors on v_2 are dominated by the RP resolution, and are estimated to be $\sim 6\%$ for central and mid-central collisions, and $\sim 10\%$ for the peripheral collisions [4].

To fix the value of b_0 , we followed the subtraction procedure of Refs. [4, 18] and assumed that Y_{jet} has zero yield at its minimum $\Delta\phi_{\text{min}}$ (ZYAM). To estimate the possible over-subtraction at $\Delta\phi_{\text{min}}$, we calculate b_0 values independently by fitting $Y_{\text{jet}}(\Delta\phi)$ to a function consisting of one near-side and two symmetric away-side Gaussians. The fitting procedure is similar to that used in [5], except that a region around π ($|\Delta\phi - \pi| < 1$) is excluded to avoid ‘‘punch-through’’ jets around π (see Fig.1). This fit accounts for the overlap of the near- and away-side Gaussians at $\Delta\phi_{\text{min}}$, and thus gives systematically lower b_0 values than that for ZYAM. We assign the differences as one-sided systematic errors on b_0 . This over-subtraction error is only significant in central collisions and at $p_T^{A,B} < 3$ GeV/c.

The per-trigger yield distributions for $p + p$ and 0-20% central Au+Au collisions are compared in Fig. 1 for various combinations of trigger and partner p_T ranges ($p_T^A \otimes p_T^B$) as indicated. The $p+p$ data show essentially Gaussian away-side peaks centered at $\Delta\phi \sim \pi$ for all p_T^A and p_T^B . In contrast, the Au+Au data show substantial shape modifications dependent on p_T^A and p_T^B . For a fixed value of p_T^A , Figs. 1(a)-(d) reveal a striking evolution from a broad, roughly flat peak to a local minimum at $\Delta\phi \sim \pi$ with side-peaks at $\Delta\phi \sim \pi \pm 1.1$. Interestingly, the location of the side-peaks in $\Delta\phi$ is roughly constant with increasing p_T^B (see also [5]). Such p_T independence is compatible with the away-side jet modification expected from a medium-induced ‘‘Mach Shock’’ [12] but disfavors models which incorporate large angle gluon radiation [9, 10], Cherenkov gluon radiation [11] or deflected jets [7, 8].

For relatively high values of $p_T^A \otimes p_T^B$, Figs. 1(e)-(h) show that the away-side jet shape for Au+Au gradually becomes peaked as for $p+p$, albeit suppressed. This ‘‘re-appearance’’ of the away-side peak seems due to a reduction of the yield centered at $\Delta\phi \sim \pi$ relative to that at $\Delta\phi \sim \pi$, rather than a merging of the peaks centered at $\Delta\phi \sim \pi \pm 1.1$. This is consistent with the dominance of dijet fragmentation at large $p_T^A \otimes p_T^B$, possibly due to jets that ‘‘punch-through’’ the medium [19] or those emitted tangentially to the medium’s surface [20].

The evolution of the away-side jet shape with p_T (cf.

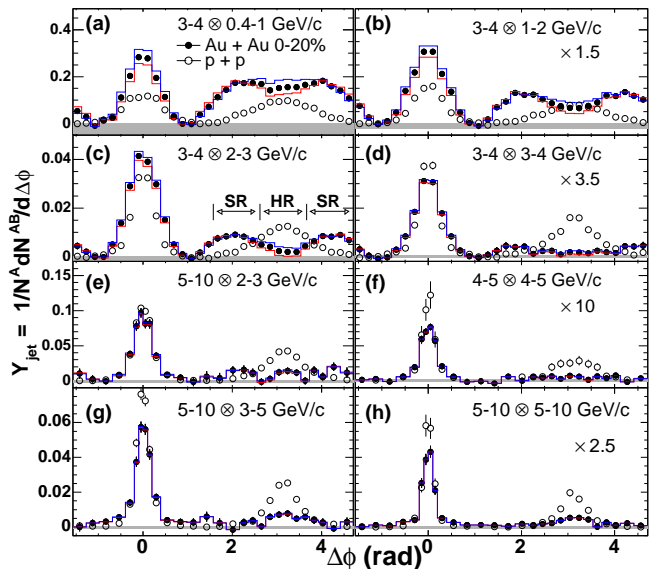


FIG. 1: Per-trigger yield versus $\Delta\phi$ for various trigger and partner p_T ($p_T^A \otimes p_T^B$), arranged by increasing pair momentum (sum of p_T^A and p_T^B), in $p + p$ and 0-20% Au+Au collisions. The Data in some panels are scaled as indicated. Solid lines (shaded bands) indicate elliptic flow (ZYAM) uncertainties. Arrows in (c) indicate ‘‘head’’ (HR) and ‘‘shoulder’’ (SR) regions.

Fig. 1) suggests separate contributions from a medium-induced component centered at $\Delta\phi \sim \pi \pm 1.1$ and a fragmentation component centered at $\Delta\phi \sim \pi$. A model independent study of these contributions can be made by dividing the away-side jet function into equal-sized ‘‘head’’ ($|\Delta\phi - \pi| < \pi/6$, HR) and ‘‘shoulder’’ ($\pi/6 < |\Delta\phi - \pi| < \pi/2$, SR) regions, as indicated in Fig. 1(c). We characterize the relative amplitude of these two regions with the ratio, R_{HS} ,

$$R_{\text{HS}} = \frac{\int_{\Delta\phi \in \text{HR}} d\Delta\phi Y_{\text{jet}}(\Delta\phi)}{\Delta\phi_{\text{HR}}} \bigg/ \frac{\int_{\Delta\phi \in \text{SR}} d\Delta\phi Y_{\text{jet}}(\Delta\phi)}{\Delta\phi_{\text{SR}}} \quad (2)$$

Since N_A in Eq.1 cancels in the ratio, R_{HS} is a pure pair variable and is symmetric *w.r.t* p_T^A and p_T^B : $R_{\text{HS}}(p_T^A, p_T^B) = R_{\text{HS}}(p_T^B, p_T^A)$. For concave and convex shapes, one expects $R_{\text{HS}} < 1$ and $R_{\text{HS}} > 1$, respectively.

Figure 2 summarizes the p_T^B dependence of R_{HS} for both $p + p$ and central Au+Au collisions in four p_T^A bins. The ratios for $p + p$ are always above one and increase with p_T^B . This reflects the narrowing of a peaked jet shape with increasing p_T^B [15]. In contrast, the ratios for Au+Au show a non-monotonic dependence on $p_T^{A,B}$. They evolve from $R_{\text{HS}} \sim 1$ for $p_T^{A,B} \lesssim 1$ GeV/c through $R_{\text{HS}} < 1$ for $1 \lesssim p_T^{A,B} \lesssim 4$ GeV/c followed by $R_{\text{HS}} > 1$ for $p_T^{A,B} \gtrsim 5$ GeV/c. These trends reflect the competition between medium-induced modification and jet fragmentation, and suggest that the latter dominates at $p_T^{A,B} \gtrsim 5$ GeV/c. The results shown in Fig. 1 indicate that, relative to $p + p$, the Au+Au yield is suppressed in

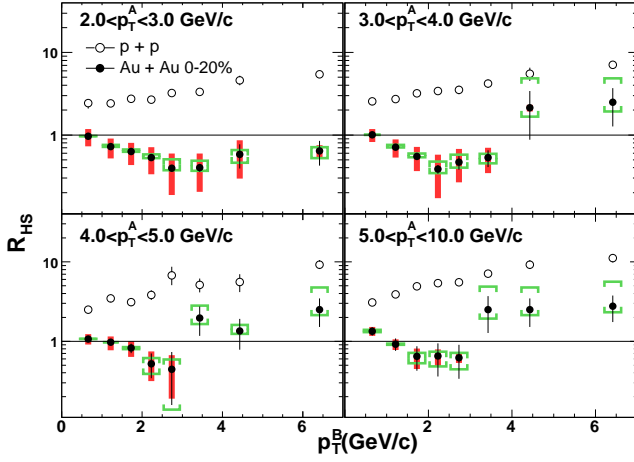


FIG. 2: R_{HS} versus p_T^B for $p + p$ (open) and Au+Au (filled) collisions for four trigger selections. Since R_{HS} is purely hadron pair variable, the result is unchanged by swapping p_T^A and p_T^B . Shaded bars (brackets) represent p_T -correlated uncertainties due to elliptic flow (ZYAM procedure).

the HR but is enhanced in the SR. We quantify this suppression/enhancement via I_{AA} , the ratio of jet yield Y_{jet} between Au+Au and $p + p$ collisions over a $\Delta\phi$ region, W , $I_{\text{AA}}^W = \int_{\Delta\phi \in W} d\Delta\phi Y_{\text{jet}}^{\text{Au+Au}} / \int_{\Delta\phi \in W} d\Delta\phi Y_{\text{jet}}^{p+p}$.

Figure 3 shows I_{AA} as a function of p_T^B for the HR and the HR+SR, respectively, in four p_T^A bins. For triggers of $2 < p_T^A < 3$ GeV/c, I_{AA} for HR+SR exceeds one at low p_T^B , but falls and crosses one at ~ 3.5 GeV/c. A similar trend is observed for the higher p_T triggers, but the enhancement (at low p_T^B) is smaller and the suppression (at high p_T^B) is stronger. The I_{AA} values in HR are lower relative to HR+SR for all $p_T^{A,B}$. For the low p_T triggers, the suppression sets in around $1 \lesssim p_T^B \lesssim 3$ GeV/c, followed by a fall-off for $p_T^B \gtrsim 4$ GeV/c. For higher p_T triggers, a constant level of $\sim 0.2 - 0.3$ is observed above ~ 2 GeV/c similar to the suppression level of inclusive hadrons [2]. These results provide clear evidence for significant yield enhancement in the SR and suppression in the HR. The data suggest that the SR reflects the dissipative processes that redistribute the energy lost in the medium; The suppression for the HR is consistent with jet quenching. However, we note that the I_{AA} values for the HR are upper limit estimates for the jet fragmentation component. This is because the HR yield includes possible contributions from the tails of the SR, as well as from bremsstrahlung gluon radiations [9].

To further explore the interplay between the HR and the SR, we focus on the intermediate p_T region, $1 < p_T^B < 5$ GeV/c, where the medium-induced component dominates the away-side yield. We characterize the inverse local slope of the partner yield in this p_T range via a truncated mean p_T , $\langle p_T' \rangle \equiv \langle p_T^B \rangle_{|1 < p_T^B < 5 \text{ GeV/c} - 1 \text{ GeV/c}}$. $\langle p_T' \rangle$ is calculated from the jet yields used to

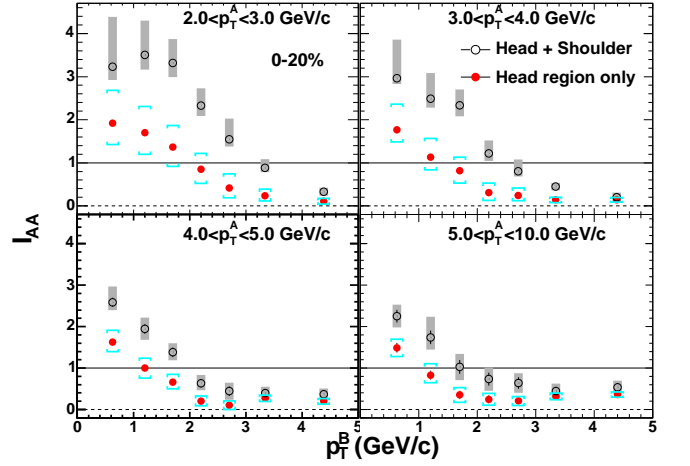


FIG. 3: I_{AA} versus p_T^B for four trigger p_T bins in HR+SR ($|\Delta\phi - \pi| < \pi/2$) and HR ($|\Delta\phi - \pi| < \pi/6$). The total systematic errors for the two regions, represented by shaded bars and brackets respectively, are strongly correlated. Grey bands around $I_{\text{AA}} = 1$ represent 14% combined uncertainty on the single particle efficiency in Au+Au and $p + p$.

make I_{AA} in Fig. 3. Fig. 4 shows the $\langle p_T' \rangle$ values for the HR, SR and a near-side region ($|\Delta\phi| < \pi/3$, NR), as a function of the number of participating nucleons, N_{part} . The $\langle p_T' \rangle$ values for NR have a weak centrality dependence. Their overall levels for $N_{\text{part}} > 100$ are 0.533 ± 0.024 , 0.605 ± 0.032 and 0.698 ± 0.040 GeV/c for the p_T^A ranges 2-3, 3-4 and 4-5 GeV/c, respectively [21]. This finding is consistent with the dominance of jet fragmentation on the near-side, i.e. a harder spectrum for partner hadrons is expected for higher p_T trigger hadrons.

A very weak centrality dependence is observed for the SR for $N_{\text{part}} \gtrsim 100$. In this case, the values for $\langle p_T' \rangle$ are lower (≈ 0.45 GeV/c) and do not depend on p_T^A . They are, however, larger than the values measured for inclusive charged hadrons (0.38 GeV/c shown by solid lines) [2]. The relatively sharp increase in $\langle p_T' \rangle$ for $N_{\text{part}} \lesssim 100$ may reflect a significant jet fragmentation contribution in peripheral collisions. In contrast, the $\langle p_T' \rangle$ values for the HR show a gradual decrease with N_{part} , starting close to that for the near-side jet, and approaches the value for the inclusive spectrum for $N_{\text{part}} \gtrsim 150$.

The different patterns observed for the yields in the HR and SR suggest a different origin for these yields. The suppression of the HR yield and the softening of its spectrum are consistent with a depletion of yield due to jet quenching. The observed HR yield could be comprised of contributions from “punch-through” jets, radiated gluons and feed-in from the SR. By contrast, the enhancement of the SR yield for $p_T^{A,B} < 4$ GeV/c suggests a remnant of the lost energy from quenched jets. However, the very weak dependence on p_T and centrality (for $N_{\text{part}} \gtrsim 100$) for its peak location and mean p_T may re-

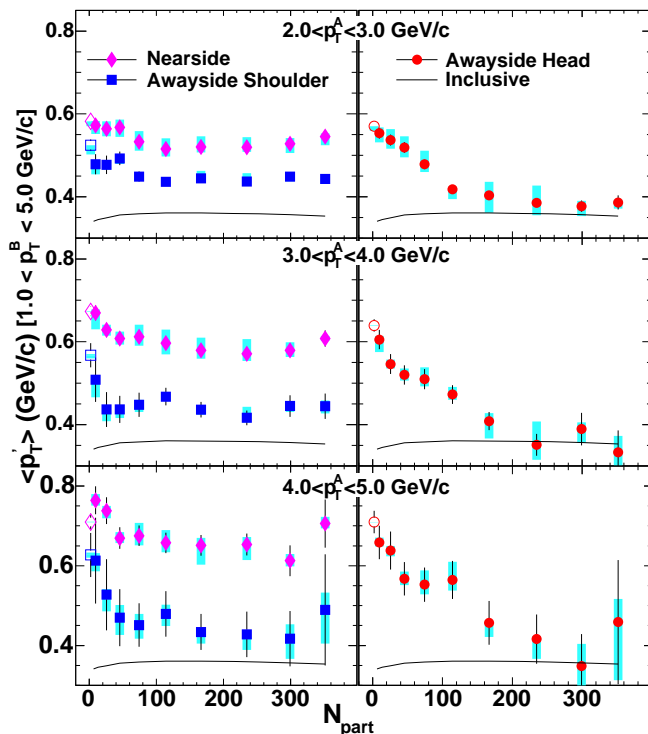


FIG. 4: Truncated mean $\langle p_T^B \rangle$ in $1 < p_T^B < 5$ GeV/c versus N_{part} for the near-side (diamonds), away-side shoulder (circles) and head (squares) regions for Au+Au (filled) and p+p (open) for three trigger p_T^A bins. Solid lines represent measured values for inclusive charged hadrons [2]. Error bars represent the statistical errors. Shaded bars represent the sum of N_{part} -correlated elliptic flow and ZYAM error.

fect an intrinsic property of the response of the medium to the energetic jets. These observations are inconsistent with simple deflected jet [7, 8] and Cherenkov gluon radiation [11] models, since both the deflection/radiation angle and jet spectra slope would depend on the p_T^A or p_T^B . However, these results are consistent with expectations for “Mach Shock” in a near-ideal hydrodynamical medium [12, 22], and thus they can be used to constrain medium transport properties such as speed of sound and viscosity to entropy ratio.

In conclusion, we have observed strong medium modification of away-side shapes and yields for jet-induced pairs in Au+Au collisions at $\sqrt{s_{NN}}=200$ GeV. The detailed dependence of these results on p_T and centrality gives strong evidence for two distinct contributions from the regions of $\Delta\phi \sim \pi$ and $\Delta\phi \sim \pi \pm 1.1$. The former is consistent with jet quenching. The latter exhibits p_T and

centrality independent shape and mean p_T , possibly reflecting an intrinsic property of the medium response to energetic jets. These results provide strong constraints on competing mechanisms for the energy transport.

We thank the staff of the Collider-Accelerator and Physics Departments at BNL for their vital contributions. We acknowledge support from the Department of Energy and NSF (U.S.A.), MEXT and JSPS (Japan), CNPq and FAPESP (Brazil), NSFC (China), MSMT (Czech Republic), IN2P3/CNRS and CEA (France), BMBF, DAAD, and AvH (Germany), OTKA (Hungary), DAE (India), ISF (Israel), KRF and KOSEF (Korea), MES, RAS, and FAAE (Russia), VR and KAW (Sweden), U.S. CRDF for the FSU, US-Hungarian NSFOTKA- MTA, and US-Israel BSF.

* PHENIX Spokesperson: jacak@skipper.physics.sunysb.edu
 † Deceased

- [1] M. Gyulassy, I. Vitev, X. N. Wang and B. W. Zhang, nucl-th/0302077; A. Kovner and U. A. Wiedemann, hep-ph/0304151.
- [2] S. S. Adler *et al.* Phys. Rev. C **69**, 034910 (2004)
- [3] J. Adams *et al.* Phys. Rev. Lett. **97**, 162301 (2006)
- [4] S. S. Adler *et al.* Phys. Rev. Lett. **97**, 052301 (2006)
- [5] A. Adare *et al.* nucl-ex/0611019.
- [6] J. Adams *et al.* Phys. Rev. Lett. **95**, 152301 (2005)
- [7] C. Chiu and R. Hwa, Phys. Rev. C **74**, 064909 (2006)
- [8] N. Armesto, C. A. Salgado and U. A. Wiedemann, Phys. Rev. Lett. **93**, 242301 (2004)
- [9] I. Vitev, Phys. Lett. B **630**, 78 (2005)
- [10] A. D. Polosa and C. A. Salgado, Phys. Rev. C **75**, 041901 (2007)
- [11] I. M. Dremin, JETP Lett. **30** (1979) 140; V. Koch, A. Majumder and X. N. Wang, Phys. Rev. Lett. **96**, 172302 (2006)
- [12] J. Casalderrey-Solana, E. V. Shuryak and D. Teaney, J. Phys. Conf. Ser. **27**, 22 (2005); hep-ph/0602183.
- [13] A. Adare *et al.* Phys. Rev. Lett. **97**, 252002 (2006)
- [14] K. Adcox *et al.* Nucl. Instrum. Meth. A **499**, 469 (2003).
- [15] S. S. Adler *et al.* Phys. Rev. C **73**, 054903 (2006)
- [16] S. S. Adler *et al.* Phys. Rev. Lett. **95**, 202001 (2005)
- [17] S. S. Adler *et al.* [PHENIX Collaboration], Phys. Rev. Lett. **91**, 182301 (2003)
- [18] N. N. Ajitanand *et al.*, Phys. Rev. C **72**, 011902 (2005)
- [19] T. Renk and K. J. Eskola, hep-ph/0610059.
- [20] C. Loizides, Eur. Phys. J. C **49**, 339 (2007)
- [21] Values at $N_{part} > 100$ are slightly lower than in $p + p$, possibly due to a contribution from a near-side “ridge” [6] in PHENIX η acceptance.
- [22] T. Renk and J. Ruppert, Phys. Rev. C **73**, 011901 (2006)